INTERNATIONAL JOURNAL FOR NUMERICAL METHODS IN FLUIDS
Int. J. Numer. Meth. Fluids 2007; **54**:1407–1423
Published online 13 February 2007 in Wiley InterScience (www.interscience.wiley.com). DOI: 10.1002/fld.1425

Volumetric methods for evaluating energy loss and heat transfer in cavity flows‡

Stuart Norris and Gordon Mallinson*, †

Department of Mechanical Engineering, The University of Auckland, Auckland, New Zealand

SUMMARY

Methods have been developed for calculating irreversible energy losses and rates of heat transfer from computational fluid dynamics solutions using volume integrations of energy dissipation or entropy production functions. These methods contrast with the more usual approach of performing first law energy balances over the boundaries of a flow domain. Advantages of the volumetric approach are that the estimates involve the whole flow domain and are hence based on more information than would otherwise be used, and that the energy dissipation or entropy production functions allow for detailed assessment of the mechanisms and regions of energy loss or entropy production.

Volume integrations are applied to the calculation of viscous losses in a lid-driven cavity flow, and to the viscous losses and heat transfer due to natural convection in a side-heated cavity. In the convection problem comparison with the entropy increase across a stationary heat conducting layer leads to a novel volume integral expression for the Nusselt number. The predictions using this method compare well with traditional surface integrals and benchmark results. Copyright © 2007 John Wiley & Sons, Ltd.

Received 3 November 2005; Revised 13 November 2006; Accepted 24 November 2006

KEY WORDS: volumetric methods; entropy production; irreversible energy loss

INTRODUCTION

The conventional approach for estimating the energy loss and heat transfer in a domain is to place a control volume around it and perform momentum and energy balances at the boundaries of the volume. An alternative approach is to estimate the irreversible losses directly. For a viscous flow energy is lost irreversibly as the fluid works against viscosity, and this loss can be represented as a volumetric energy sink by the viscous dissipation function. This is appropriate, even when

*Correspondence to: Gordon Mallinson, Department of Mechanical Engineering, The University of Auckland, Auckland, New Zealand.
†E-mail: g.mallinson@auckland.ac.nz
‡This is the second part of paper fld.1193, originally submitted as part of the already published special issue FHTC [50/11].

Copyright © 2007 John Wiley & Sons, Ltd.

the flow can be regarded as being isothermal, in which case the viscous dissipation is insufficient to significantly influence the distribution of specific enthalpy in the fluid. However, as discussed later, viscous dissipation is more likely to influence a second law analysis and is hence relevant for the estimation of irreversible losses.

To demonstrate the utility of volumetric expressions they have been applied to two well-studied flows, the lid-driven cavity, and natural convection in a differentially heated cavity. The lid-driven cavity flow [1, 2] is used to demonstrate how the work expended against the viscosity of the fluid can be estimated by both boundary integration of the product of velocity and shear stress on the sliding surface, and also by the volume integration of the viscous dissipation function. The natural convection flow [3] demonstrates how volume integrations produce estimates for the Nusselt number that can be compared with values obtained by calculating the heat flux at the surface.

MATHEMATICAL MODELLING

For the modelled flows the fluid motion and heat transfer are assumed to be well represented by the Boussinesq approximation. Apart from the influence of thermal expansion on the buoyancy term, the fluid is assumed to be incompressible and have constant properties. Equations (1) and (2) are the relevant versions of the momentum and energy equations, respectively. The only departure from the usual treatment of such flows is the inclusion of the viscous dissipation term in the energy equation.

$$\frac{\mathrm{D}\mathbf{u}}{\mathrm{D}t} = -\frac{\nabla P}{\rho} - \beta(T - T_0)\mathbf{g} + \nu\nabla^2\mathbf{u} \tag{1}$$

$$\frac{\mathrm{D}T}{\mathrm{D}t} = \frac{k}{\rho c_p}\nabla^2 T + \frac{\nu}{c_p}\Phi \tag{2}$$

The function Φ is the viscous dissipation function which for a three-dimensional Cartesian coordinate system has the form

$$\Phi = 2\left\{\left(\frac{\partial u}{\partial x}\right)^2 + \left(\frac{\partial v}{\partial y}\right)^2 + \left(\frac{\partial w}{\partial z}\right)^2\right\} + \left(\frac{\partial v}{\partial x} + \frac{\partial u}{\partial y}\right)^2 + \left(\frac{\partial w}{\partial y} + \frac{\partial v}{\partial z}\right)^2 + \left(\frac{\partial u}{\partial z} + \frac{\partial w}{\partial x}\right)^2 - \frac{2}{3}\left(\frac{\partial u}{\partial x} + \frac{\partial v}{\partial y} + \frac{\partial w}{\partial z}\right)^2 \tag{3}$$

In a two-dimensional coordinate system Φ reduces to

$$\Phi = 2\left\{\left(\frac{\partial u}{\partial x}\right)^2 + \left(\frac{\partial v}{\partial y}\right)^2\right\} + \left(\frac{\partial v}{\partial x} + \frac{\partial u}{\partial y}\right)^2 - \frac{2}{3}\left(\frac{\partial u}{\partial x} + \frac{\partial v}{\partial y}\right)^2 \tag{4}$$

The equations can be written in non-dimensional forms by choosing appropriate reference quantities for all the variables in the governing equations. Equations (5) and (6) are the result of choosing a single characteristic length L, a reference velocity U_{ref}, using ρU_{ref}^2 as a reference for pressure and representing the absolute temperature by $T = T_0 + \Delta T\,\theta$.

$$\frac{\mathrm{D}\mathbf{u}}{\mathrm{D}t} = -\nabla P - \frac{Ra}{Re}\theta\hat{\mathbf{g}} + \frac{1}{Re}\nabla^2\mathbf{u} \tag{5}$$

Copyright © 2007 John Wiley & Sons, Ltd.

DOI: 10.1002/fld

$$\frac{\mathrm{D}\theta}{\mathrm{D}t} = \frac{1}{Pe}[\nabla^2\theta + Ec\,Pr\Phi] \tag{6}$$

Conventional practice is followed, whereby it is understood that the variables appearing in equations containing non-dimensional numbers have been scaled whereas those containing dimensional parameters have not. *Re* is the Reynolds number, *Ra* the Rayleigh number, *Pe* the Peclet number, *Pr* the Prandtl number, and *Ec* the Eckert number (see Appendix A). The product *Ec Pr*, which indicates the relative strength of viscous dissipation to conduction in the transport of energy, is called the Brinkmann number.

For a forced flow, such as that in a lid-driven cavity, there is an obvious choice for U_{ref}. For a natural convection flow, a choice that is often made is

$$U_{\mathrm{ref}} = \frac{k}{\rho c_p L} = \frac{\alpha}{L} \Rightarrow Pe = 1 \tag{7}$$

If this choice is made, Equations (5) and (6) become,

$$\frac{\mathrm{D}\mathbf{u}}{\mathrm{D}t} = -\nabla P - Ra\,Pr\theta\hat{\mathbf{g}} + Pr\nabla^2\mathbf{u} \tag{8}$$

$$\frac{\mathrm{D}\theta}{\mathrm{D}t} = \nabla^2\theta + Ec\,Pr\Phi \tag{9}$$

and the Eckert and Brinkman numbers are

$$Ec = \frac{U_{\mathrm{ref}}^2}{c_p\Delta T} = \frac{\alpha^2}{c_p L^2\Delta T}, \quad Ec\,Pr = \frac{\alpha v}{c_p L^2\Delta T} \tag{10}$$

Note that in the convection example discussed in this paper, the scaled maximum velocities will not necessarily be of order unity and this will influence the value of *Ec Pr* at which viscous dissipation becomes important.

IRREVERSIBLE ENERGY LOSSES AND ENTROPY PRODUCTION

For many common flow situations the Brinkmann number is small and the viscous dissipation function can be dropped from Equation (6) or (9). This means that the heat released as work is done against viscosity does not influence the flow and temperature fields. The energy is, nevertheless, lost irreversibly from the fluid and the rate of loss can be estimated by integrating the viscous dissipation function over the volume occupied by the fluid

$$\dot{Q}_{\mathrm{irrev}} = \mu\int_V \Phi\,\mathrm{d}v \tag{11}$$

For an open control volume surrounding a steady flow the conservation of energy can be expressed as

$$\dot{Q} - \dot{W} = \Delta\dot{E} \tag{12}$$

where $\dot{Q}$ is the heat transfer into the volume, $\dot{W}$ is the rate of work done by the fluid on its surroundings and $\Delta\dot{E}$ and is the total rate at which energy leaves the volume. For the processes considered here, $\Delta\dot{E}$ is a summation over all openings of the outwards energy flow rates.

Copyright © 2007 John Wiley & Sons, Ltd.

DOI: 10.1002/fld

The rate of heat generation by viscous dissipation, $\dot{Q}_{\text{irrev}}$, is eventually transferred across the boundaries and is lost by the fluid. It is therefore a negative contribution to $\dot{Q}$ in Equation (12).

Following a second law elemental control volume analysis (e.g. [4, pp. 99–101]), the volumetric rate of entropy production in a fluid with constant properties can be written as

$$\dot{S}''' = \frac{1}{T}\nabla\cdot\mathbf{q} - \frac{1}{T^2}\mathbf{q}\cdot\nabla T + \rho\frac{\mathrm{D}s}{\mathrm{D}t}$$

$$= -\frac{1}{T}k\nabla^2 T + \frac{k}{T^2}(\nabla T)^2 + \rho\frac{\mathrm{D}s}{\mathrm{D}t} \tag{13}$$

The canonical relation $\mathrm{d}e = T\,\mathrm{d}s - P\mathrm{d}(1/\rho)$ leads to

$$\rho\frac{\mathrm{D}s}{\mathrm{D}t} = \frac{\rho}{T}\frac{\mathrm{D}e}{\mathrm{D}t} - \frac{P}{\rho T}\frac{\mathrm{D}\rho}{\mathrm{D}t} \tag{14}$$

For incompressible flow, $\mathrm{D}\rho/\mathrm{D}t = 0$ and $\mathrm{D}e/\mathrm{D}t = c_p\mathrm{D}T/\mathrm{D}t$. Substituting these relationships in (14) and using the energy equation (2),

$$\rho\frac{\mathrm{D}s}{\mathrm{D}t} = \frac{\rho c_p}{T}\frac{\mathrm{D}T}{\mathrm{D}t} = \frac{k}{T}\nabla^2 T + \frac{\mu\Phi}{T} \tag{15}$$

Although derived for incompressible flow here, Equation (15) also holds for compressible flows, e.g. Equation 6.3.9 in [5] or Equation 3.4.11 in [6].

Substituting (15) into (13) leads to

$$\dot{S}''' = \frac{k}{T^2}(\nabla T)^2 + \frac{\mu\Phi}{T} \tag{16}$$

The non-dimensional form of Equation (16) is

$$\frac{\dot{S}'''}{\dot{S}'''_{\text{ref}}} = \frac{\varepsilon^2}{1+\varepsilon\theta}\left[\frac{1}{1+\varepsilon\theta}(\nabla\theta)^2 + \frac{Ec\,Pr}{\varepsilon}\Phi\right] : \dot{S}'''_{\text{ref}} = \frac{k}{L^2}, \quad \varepsilon = \frac{\Delta T}{T_0} \tag{17}$$

As recognized by others [4, 7], the immediate implication of (17) is that viscous dissipation is more likely to play a role in the production of entropy than it does in the conservation of energy because the ratio between the viscous dissipation and heat conduction terms is modified by the temperature ratio ε, which is often small.

LOSSES IN LID-DRIVEN CAVITY FLOW

Possibly the simplest flow to model is that in a two-dimensional lid-driven cavity, a schematic of which is given in Figure 1. The cavity is of unit dimensions in the x and y directions, with the upper surface being driven to the right at a prescribed velocity. To prevent the velocity being multi-valued in the upper two corners of the cavity, as occurs with the conventional driven cavity problem where the velocity of driven wall is constant along it's length [1], the regularized (i.e. homogeneous) boundary condition of Shen [2] was used where the velocity of the upper surface varies as $U(x) = 16x^2(1-x)^2$ over the range $0 \leqslant x \leqslant 1$, being at a maximum at the centre of the cavity and decreasing to zero in the corners.

Copyright © 2007 John Wiley & Sons, Ltd.

DOI: 10.1002/fld

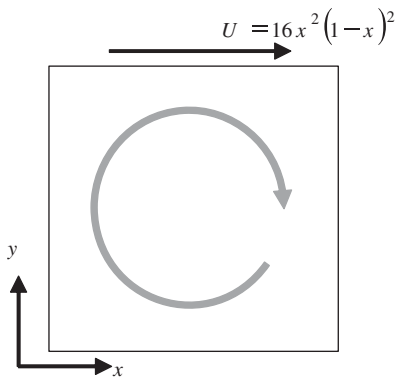

Figure 1. The regularized lid-driven cavity.

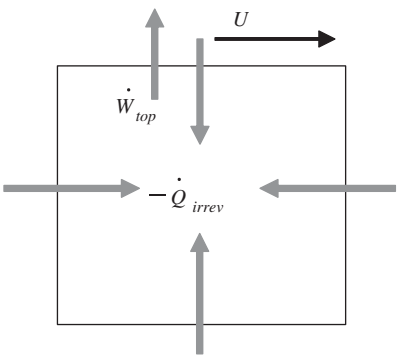

Figure 2. Work and heat flows for the lid-driven cavity.

A first law analysis for the domain gives

$$-\dot{W}_{\text{top}} - \dot{Q}_{\text{irrev}} = 0 \tag{18}$$

the sign convention for the work and heat flows being given in Figure 2.

The only work performed on the cavity is that by the motion of the lid, which in dimensional terms is

$$\dot{W}_{\text{top}} = -\mu \int_0^1 U(x) \left.\frac{\partial u}{\partial y}\right|_{y=1} \mathrm{d}x \tag{19}$$

For a constant viscosity the irreversible energy loss due to the viscous dissipation is

$$\dot{Q}_{\text{irrev}} = \mu \int_0^1 \int_0^1 \Phi \,\mathrm{d}x\,\mathrm{d}y = \mu \int_0^1 \int_0^1 \left[2\left\{ \left(\frac{\partial u}{\partial x}\right)^2 + \left(\frac{\partial v}{\partial y}\right)^2 \right\} + \left(\frac{\partial v}{\partial x} + \frac{\partial u}{\partial y}\right)^2 - \frac{2}{3}\left(\frac{\partial u}{\partial x} + \frac{\partial v}{\partial y}\right)^2 \right] \mathrm{d}x\,\mathrm{d}y \tag{20}$$

Copyright © 2007 John Wiley & Sons, Ltd.

DOI: 10.1002/fld

LOSSES AND HEAT TRANSFER IN BUOYANT FLOW

For natural convection flow, the driving force is thermally induced buoyancy. The analysis of the irreversibilities in the flow must include the temperature and heat transfer within the fluid.

It is useful for the analysis that follows to apply the integration of the volumetric entropy generation function (16) to calculate the entropy produced by heat conduction through a solid slab. Using the notation in Figure 3,

$$T = T_{\mathrm{h}} + \frac{T_{\mathrm{c}} - T_{\mathrm{h}}}{L} x \quad \text{and} \quad \nabla T = \frac{T_{\mathrm{c}} - T_{\mathrm{h}}}{L} \tag{21}$$

The expression for volumetric entropy generation is

$$\dot{S}''' = \frac{k(T_{\mathrm{c}} - T_{\mathrm{h}})}{(LT_{\mathrm{h}} + (T_{\mathrm{c}} - T_{\mathrm{h}})x)^2} \tag{22}$$

The entropy production rate is then given by

$$\dot{S} = A \int_0^L \dot{S}''' \, \mathrm{d}x = \frac{Ak(T_{\mathrm{h}} - T_{\mathrm{c}})^2}{LT_{\mathrm{h}}T_{\mathrm{c}}} \tag{23}$$

The rate of heat transfer through the slab is, of course, given by

$$\dot{Q} = \frac{Ak(T_{\mathrm{h}} - T_{\mathrm{c}})}{L} \tag{24}$$

so that the entropy production rate is related to the heat transfer rate by

$$\dot{S} = \dot{Q} \frac{(T_{\mathrm{h}} - T_{\mathrm{c}})}{T_{\mathrm{h}}T_{\mathrm{c}}} = \dot{Q} \left(\frac{1}{T_{\mathrm{c}}} - \frac{1}{T_{\mathrm{h}}} \right) \tag{25}$$

The last result could also have been obtained by applying the second law directly to a control volume around the slab.

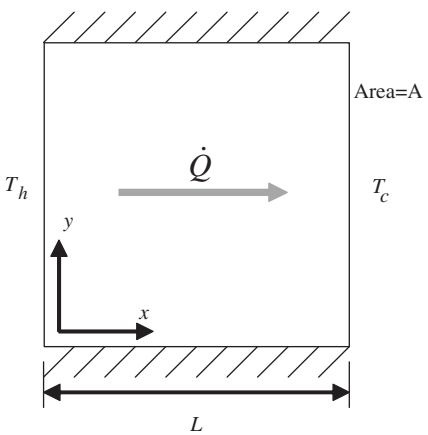

Figure 3. Notation for entropy production for heat flow through a stationary domain.

Copyright © 2007 John Wiley & Sons, Ltd.

DOI: 10.1002/fld

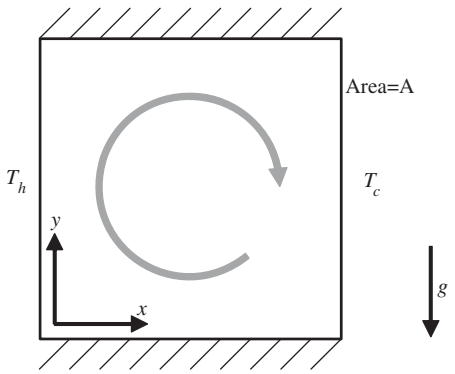

Figure 4. Natural convection in a cavity heated from the side, with adiabatic upper and lower walls.

Consider now convection in a box that has vertical isothermal hot and cold boundaries of area A and separated by a distance L. The heat transfer is in the x direction and is the result of buoyancy-induced convection, as shown in Figure 4. The rate of entropy production is

$$\dot{S} = k \int_V \left[\left(\frac{\nabla T}{T} \right)^2 + \frac{\mu}{k} \frac{\Phi}{T} \right] \mathrm{d}v \tag{26}$$

Equation (26) represents the total rate of entropy production in the cavity. It is usual to separate the two mechanisms of entropy production and associate only the thermal term with heat transfer [4]. However, in the convection problem the only energy transport across a control volume surrounding the cavity is by heat transfer. Hence, the viscous dissipation is included in (26).

Although the rate of entropy production is of interest in its own right, it can have a more useful interpretation in the present context if it is related by Equation (25) to the heat transfer rate by conduction through a stationary layer having the same dimensions. Equating (25) and (26) leads to

$$\dot{Q} = \frac{k T_\mathrm{h} T_\mathrm{c}}{(T_\mathrm{h} - T_\mathrm{c})} \int_V \left[\left(\frac{\nabla T}{T} \right)^2 + \frac{\mu}{k} \frac{\Phi}{T} \right] \mathrm{d}v \tag{27}$$

Equation (27) is a volume integration that yields the rate of heat transfer through the layer. A heat transfer coefficient can be recovered using

$$h = \frac{\dot{Q}}{A(T_\mathrm{h} - T_\mathrm{c})} = \frac{k T_\mathrm{h} T_\mathrm{c}}{A(T_\mathrm{h} - T_\mathrm{c})^2} \int_V \left[\left(\frac{\nabla T}{T} \right)^2 + \frac{\mu}{k} \frac{\Phi}{T} \right] \mathrm{d}v \tag{28}$$

The Nusselt number can now be recovered by multiplying (28) by L/k or remembering that for this convection scenario, the Nusselt number is simply the ratio of the rate of heat transfer to that which occurs when there is no fluid motion

$$Nu = \frac{\dot{Q} L}{k(T_\mathrm{h} - T_\mathrm{c})} = \frac{L T_\mathrm{h} T_\mathrm{c}}{A(T_\mathrm{h} - T_\mathrm{c})^2} \int_V \left[\left(\frac{\nabla T}{T} \right)^2 + \frac{\mu}{k} \frac{\Phi}{T} \right] \mathrm{d}v \tag{29}$$

Copyright © 2007 John Wiley & Sons, Ltd.

DOI: 10.1002/fld

In terms of non-dimensional variables when $T_0 = T_c$ and $\Delta T = T_h - T_c$

$$Nu = (1+\varepsilon)\int_V \left[\left(\frac{\nabla\theta}{1+\varepsilon\theta}\right)^2 + \frac{EcPr}{\varepsilon}\frac{\Phi}{1+\varepsilon\theta}\right]\mathrm{d}v \tag{30}$$

When the viscous dissipation can be neglected, the Nusselt number is given by

$$Nu = (1+\varepsilon)\int_V \left(\frac{\nabla\theta}{1+\varepsilon\theta}\right)^2 \mathrm{d}v \tag{31}$$

When ε is very small

$$Nu \approx \int_V (\nabla\theta)^2\,\mathrm{d}v \tag{32}$$

APPLICATION OF THE VOLUMETRIC METHODS

To model the flows two computer codes were used, one that uses a structured Cartesian mesh, the second which uses an unstructured grid. EHOA [8] is a finite volume code that uses SIMPLE velocity–pressure coupling [9] and Rhie–Chow velocity interpolation [10] on a structured collocated mesh. For the current study, the velocity and temperature fields were solved on a regular hexahedral mesh. ALE [11] is an unstructured finite volume code that uses a MAC [12] coupling scheme on a mesh of Voronoi cells. Both codes used double precision (i.e. 64 bit) arithmetic, and all calculations iterated until the RMS residuals were reduced by eight orders of magnitude. Solutions were calculated using second-order central differencing, and meshes varied in size from 32^2 to 256^2 cells. Typical meshes for the two flow solvers, used for the 32^2 calculations, are shown in Figure 5.

Volumetric and surface integrals were both evaluated using a second-order finite volume discretization in a manner that was consistent, in terms of global conservation, with the flow solvers used. For the work performed by the wall in the lid-driven cavity problem, the contribution

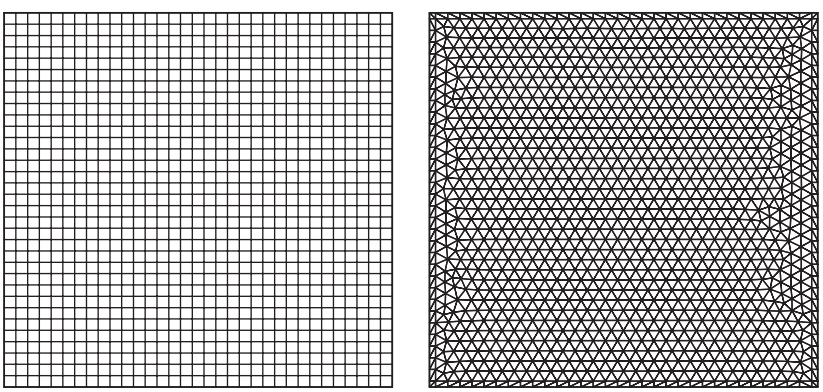

Figure 5. Typical structured and unstructured meshes used by the EHOA and ALE codes, respectively.

Copyright © 2007 John Wiley & Sons, Ltd.

DOI: 10.1002/fld

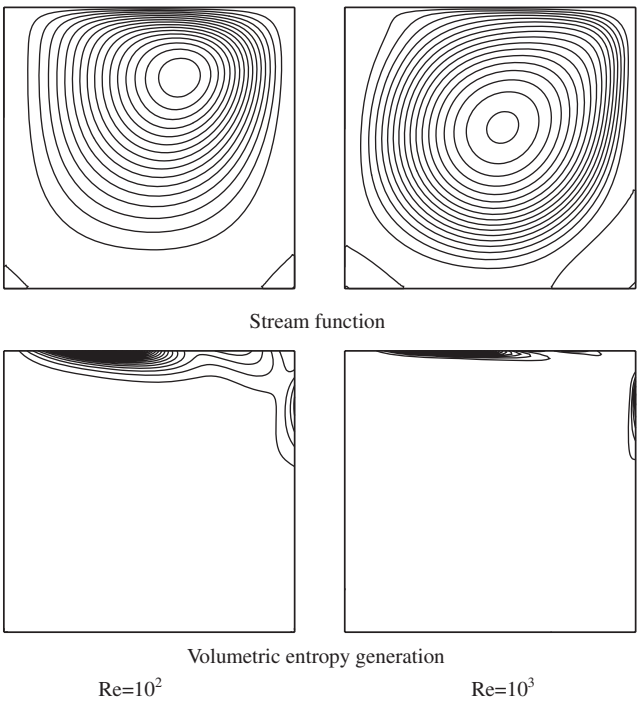

Figure 6. Contour plots of stream function and volumetric entropy generation dissipation for the driven cavity flow. Solutions calculated using EHOA on a 128^2 mesh.

from the boundary of a single finite volume cell adjacent to the upper surface is

$$-w_{\mathrm{i}} \approx \mu u_{\mathrm{b}} \frac{u_{\mathrm{b}} - u_{\mathrm{i}}}{\Delta y} \Delta x \tag{33}$$

where the subscript b signifies a value on the boundary of the domain, the subscript i that at the centre of the cell inside the domain, Δy the distance from the cell centre to the boundary, and Δx the width of the cell. The surface integral was calculated by summing over all boundary cells. Similarly, when evaluating the Nusselt number for the natural convection problem, the heat transfer by conduction into a single finite volume at the sidewall of the cavity is

$$q_{\mathrm{i}} \approx k \frac{T_{\mathrm{b}} - T_{\mathrm{i}}}{\Delta x} \Delta y \tag{34}$$

with the integral for each wall being calculated by a simple summation over all cells.

The irreversible loss given by (20) was evaluated by calculating the cell centred gradients of velocity, evaluating the cell viscous dissipation using these values, and integrating by multiplying by the cell volume and summing over the cavity. Similarly, the expression for the Nusselt number in (32) was evaluated by calculating the cell centre temperature gradient and integrating by multiplying by the cell volumes and summing over the domain.

Copyright © 2007 John Wiley & Sons, Ltd.

DOI: 10.1002/fld

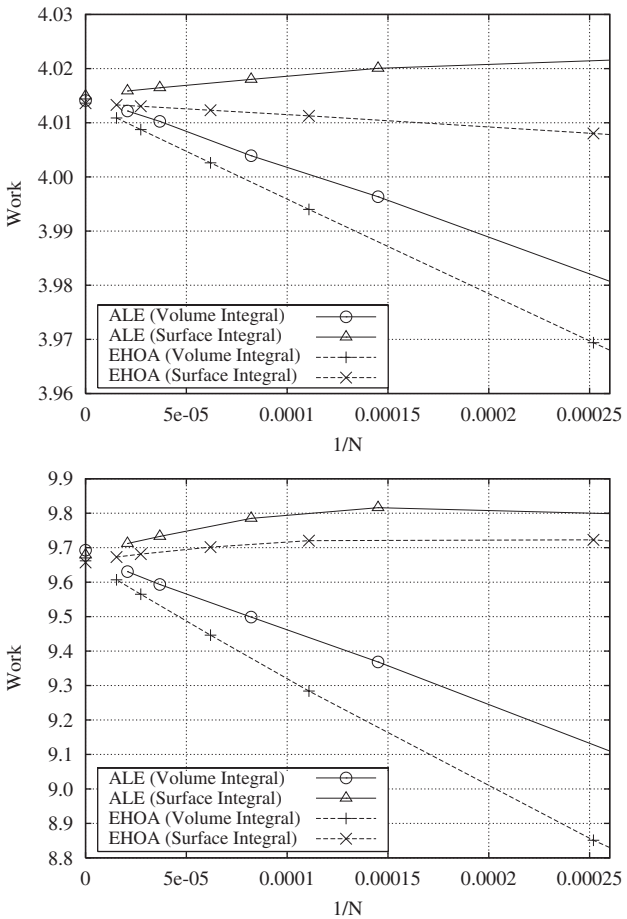

Figure 7. Non-dimensional work for the driven cavity, plotted as a function of the reciprocal of the number of finite volumes in the domain. Plotted for flows at $Re = 10^2$ (top) and 10^3 (bottom).

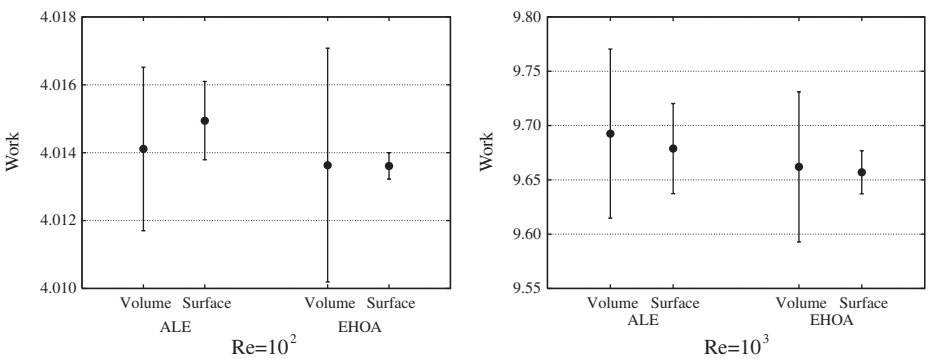

Figure 8. Extrapolated values of non-dimensional work for the driven cavity.

Copyright © 2007 John Wiley & Sons, Ltd.

DOI: 10.1002/fld

Table I. Raw values for the calculated volumetric and surface dimensionless work term for the driven cavity, together with the values calculated using Richardson extrapolation and the calculated order of convergence.

	ALE $Re = 10^2$		ALE $Re = 10^3$	
	Volumetric	Surface	Volumetric	Surface
$N = 12174$	4.00391	4.01800	9.49872	9.78503
$N = 27164$	4.01026	4.01646	9.59311	9.73280
$N = 48112$	4.01218	4.01587	9.63073	9.71215
Extrapolated	4.01411	4.01494	9.69258	9.67882
Error bounds	± 0.00241	± 0.00116	± 0.07781	± 0.04153
Order of convergence	2.42	1.74	1.66	1.69
GCI (%)	0.06	0.03	0.80	0.43
	EHOA $Re = 10^2$		EHOA $Re = 10^3$	
	Volumetric	Surface	Volumetric	Surface
$N = 16129$	4.00261	4.01232	9.44632	9.70168
$N = 36481$	4.00874	4.01305	9.56499	9.68138
$N = 65025$	4.01088	4.01330	9.60689	9.67287
Extrapolated	4.01363	4.01361	9.66192	9.65696
Error bounds	± 0.00344	± 0.00039	± 0.06918	± 0.01986
Order of convergence	1.99	2.03	1.96	1.48
GCI (%)	0.09	0.01	0.72	0.21

LID-DRIVEN CAVITY FLOW

The driven cavity flow was calculated for two different Reynolds numbers $Re = 10^2$ and 10^3, using the regularized boundary condition of Shen [2] shown in Figure 1. The work done on the cavity was evaluated using the surface integral given in (19) and the volumetric integral of viscous dissipation given in (20), the calculated values being expressed in non-dimensional form using a scaling of $\dot{Q}_{\text{ref}} = \mu U_{\text{ref}}^2 L$. The EHOA code calculated upon a regular Cartesian mesh, whilst ALE used an unstructured mesh with uniform boundary mesh spacing. Contour plots for the stream function and entropy generation are given in Figure 6.

In Figure 7 the calculated power dissipation is plotted as a function of the reciprocal of the number of finite volume cells within the interior of the cavity, with the values estimated using Richardson extrapolation being given in Figure 8, the error bars being calculated using the techniques described by Celik [13]. The raw data from the three finest meshes are listed in Table I together with the values calculated using Richardson extrapolation, the order of the mesh convergence, and the grid convergence index (GCI) [13]. With refinement of the mesh the solutions for both codes and both calculation methods converge to the same solution, within the estimated error bounds, although the order of the convergence varies despite both the solvers and the integration methods being nominally second-order accurate. For both solvers the surface integral estimates of work have tighter error bounds.

The contour plots of the distribution of the viscous dissipation function in Figure 6 indicate that the energy is lost in the shear layers adjacent to the lid and the upper part of the downstream

Copyright © 2007 John Wiley & Sons, Ltd.

DOI: 10.1002/fld

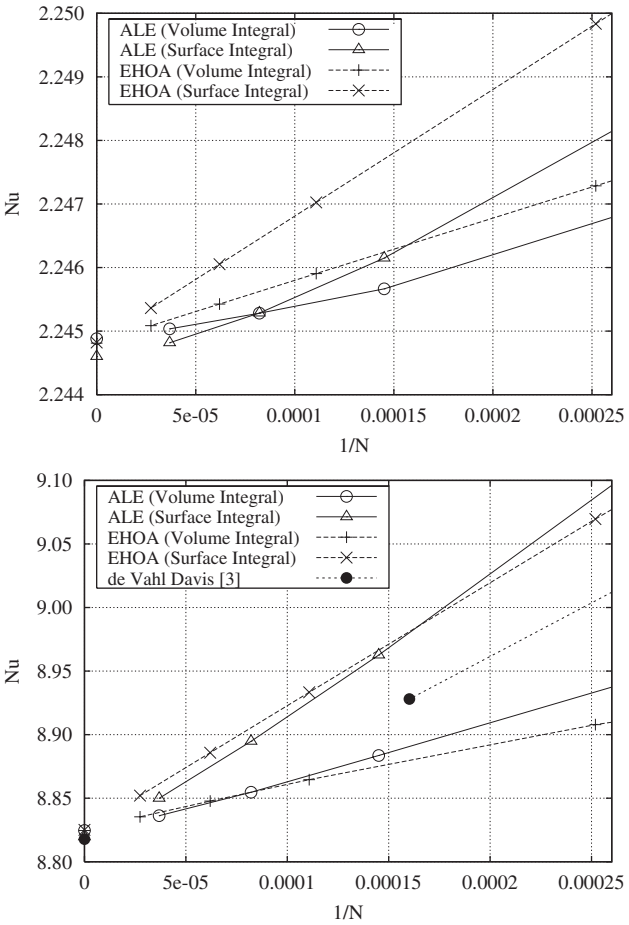

Figure 9. Nusselt number for the natural convection flow in a side-heated cavity, plotted as a function of the reciprocal of the number of finite volumes in the domain. Plotted for flows at $Ra = 10^4$ (top) and 10^6 (bottom).

wall where the fluid is pushed against the boundary. As the Reynolds number is increased the dissipation becomes concentrated in the boundary layer, and the error in the calculated power loss increases for the volume and the surface integral methods alike. The overall concentration of the dissipation in the cavity boundary layers suggests that inadequate resolution of the boundary layer will affect the calculation of the power loss for both surface and volume integrals.

CONVECTION IN A CAVITY HEATED FROM THE SIDE

To demonstrate the use of the volumetric methods in the calculation of the heat transfer in a convective flow, a standard benchmark natural convection flow was calculated for air (having a

Copyright © 2007 John Wiley & Sons, Ltd.

DOI: 10.1002/fld

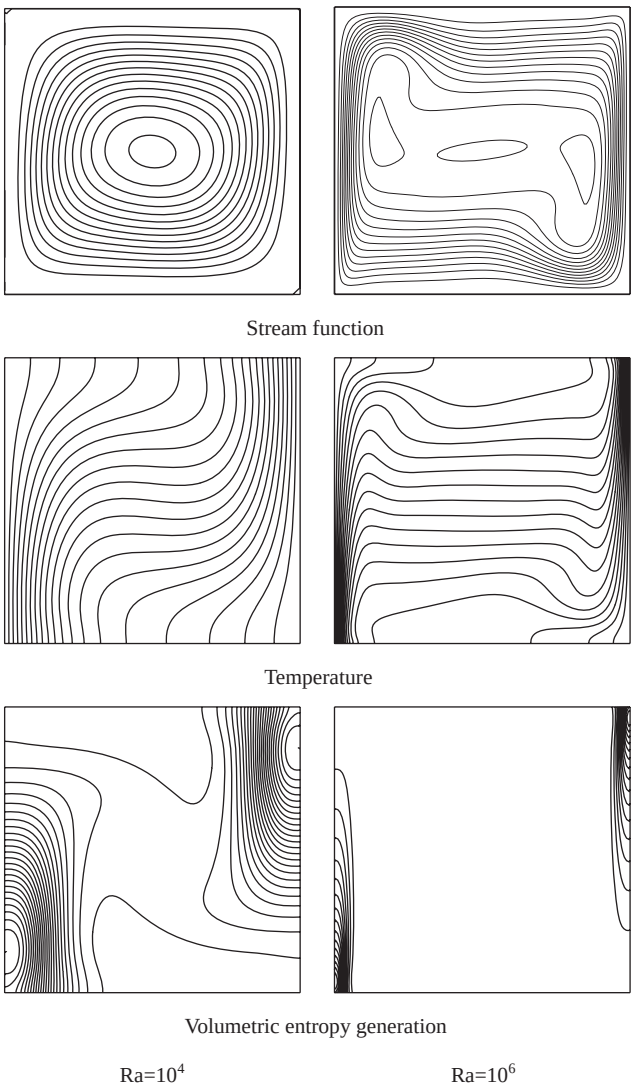

Figure 10. Contour plots of stream function, temperature and volumetric entropy generation for the side headed cavity. Solutions calculated using EHOA on a 128^2 mesh.

Prandtl number of $Pr = 0.71$) in a square cavity with isothermal vertical and adiabatic horizontal boundaries [3] (see Figure 4). The problem was solved using EHOA and ALE on the same meshes used for the driven cavity problem described above, at Rayleigh numbers of $Ra = 10^4$ and 10^6. The Nusselt numbers were calculated by estimating the conduction from the walls *via* a second-order approximation to the temperature gradient (34), and by solving the volume integral (32) evaluated by summing the cell centre gradients over the domain. Contour plots for the stream function, temperature and entropy generation are given in Figure 10.

Copyright © 2007 John Wiley & Sons, Ltd.

DOI: 10.1002/fld

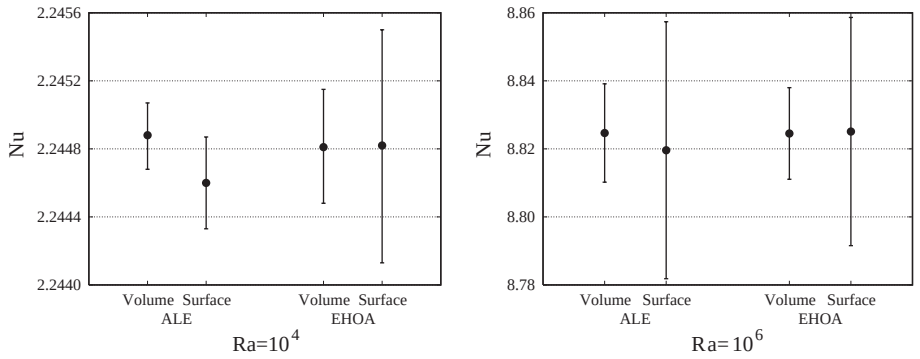

Figure 11. Extrapolated values of Nusselt number for the natural convection problem.

Table II. Raw values for the calculated volumetric and surface Nusselt number for the natural convection problem, together with the values calculated using Richardson extrapolation and the calculated order of convergence.

	ALE $Ra = 10^4$		ALE $Ra = 10^6$	
	Volumetric	Surface	Volumetric	Surface
$N = 6891$	2.24567	2.24615	8.86360	8.96259
$N = 12174$	2.24528	2.24528	8.85467	8.89475
$N = 27164$	2.24504	2.24482	8.83625	8.84993
Extrapolated	2.24488	2.24460	8.82467	8.81960
Error bounds	± 0.00020	± 0.00027	± 0.01445	± 0.03778
Order of convergence	2.35	2.87	2.37	2.26
GCI (%)	0.01	0.01	0.16	0.43
	EHOA $Ra = 10^4$		EHOA $Ra = 10^6$	
	Volumetric	Surface	Volumetric	Surface
$N = 9025$	2.24591	2.24703	8.86454	8.93334
$N = 16129$	2.24543	2.24605	8.84774	8.88580
$N = 36481$	2.24509	2.24536	8.83532	8.85202
Extrapolated	2.24481	2.24482	8.82453	8.82510
Error bounds	± 0.00034	± 0.00068	± 0.01347	± 0.03355
Order of convergence	1.99	2.00	1.88	1.99
GCI (%)	0.02	0.03	0.15	0.38

Figure 9 shows the mesh convergence of the estimates of the Nusselt number for cavities at $Ra = 10^4$ and 10^6, together with the benchmark values from [3]. The extrapolated values with estimates of the error range are shown in Figure 11, and the raw values, extrapolated values, and order of the mesh convergence are given in Table II. As with the driven cavity data, all our extrapolated values estimates agreed within the estimated error range. The extrapolated value for the Nusselt number at $Ra = 10^6$ agrees well with the benchmark solution, but at $Ra = 10^4$ it does

Copyright © 2007 John Wiley & Sons, Ltd.

DOI: 10.1002/fld

not, so much so that the benchmark value of $Nu = 2.238$ could not be plotted on the same graph. This may be due to the relatively course mesh used for the calculations of the $Ra = 10^4$ flow in the benchmark, which was only refined to a mesh of 40^2 points, as opposed to the current calculations which were refined to a mesh of 192^2 cells.

As with the driven cavity test case both the volumetric and surface integral calculations for Nusselt number exhibited approximately second-order mesh convergence. However, unlike the driven cavity case the volumetric estimate has a smaller error bound than that estimated by the surface integral.

Contour plots of the stream function, temperature and volumetric entropy generation are given in Figure 10. Compared to the driven cavity, the integrand for the entropy based heat transfer estimate is significant over a larger part of the cavity. As with the driven cavity flow, the entropy generation is concentrated at the boundaries of the domain the error in both the volume and surface integration estimates for Nusselt number increase.

CONCLUSIONS

Volume-based methods for estimating irreversible energy losses and heat transfer rates from CFD solutions have been presented and applied to a lid-driven cavity and to natural convection in a cavity heated from the side. The volumetric methods were shown to be consistent with those based on surface integrations of heat and work transfers across the domain boundaries. Neither the volumetric or surface methods were shown to be superior across all test cases, having similar orders of accuracy and error ranges. However, a plot of the fields used in the volumetric methods allows an identification of regions that contribute to fluid losses, something that is not apparent from the integral values given by the surface integral methods. The volumetric methods thus provide a valuable new tool in the study of flow fields.

APPENDIX A: NOMENCLATURE

A	area, m^2
c_P	constant pressure specific heat, $\mathrm{J/kg\,K}$
e	specific internal energy, J/kg
E	internal energy, J
Ec	Eckert number, $U^2/c_p\Delta T$
$\mathbf{g}$	acceleration due to gravity, $\mathrm{m/s}^2$
GCI	grid convergence index
k	thermal conductivity, W/mK
L	length scale, m
P	pressure, $\mathrm{N/m}^2$
Pe	Peclet number, UL/α
Pr	Prandtl number, ν/α
Nu	Nusselt number, $qL/k\Delta T$
$\mathbf{q}$	heat flux, $\mathrm{W/m}^2$
$\dot{Q}$	heat transfer, W
$\dot{Q}_{\mathrm{irrev}}$	rate of irreversible heat loss, W
$\dot{Q}_{\mathrm{ref}}$	reference rate of energy loss, $\mu U_{\mathrm{ref}}^2 L$, W

Copyright © 2007 John Wiley & Sons, Ltd.

DOI: 10.1002/fld

Ra	Rayleigh number, $g\beta\Delta T L^3/\nu\alpha$
Re	Reynolds number, UL/ν
s	specific entropy, J/kg K
$\dot{S}'''$	volumetric rate of entropy generation, W/km^3
$\dot{S}'''_{\text{ref}}$	reference volumetric rate of entropy generation, W/km^3
S	entropy, J/K
t	time, s
T	temperature, K
T_0	reference temperature, K
$\mathbf{u}$	velocity vector, m/s
u	x component of velocity, m/s
U_{ref}	reference velocity, m/s
v	y component of velocity, m/s
V	volume, m^3
w	z component of velocity, m/s
W	work, W
x	horizontal axis, m
y	vertical axis, m
α	thermal diffusivity, $k/\rho c_p$
β	coefficient for volumetric expansion for temperature, 1/K
ε	temperature ratio, $\Delta T/T_0$
θ	non-dimensional temperature, $(T - T_0)/\Delta T$
μ	dynamic viscosity, Ns/m^2
ν	kinematic viscosity, μ/ρ
ρ	density, kg/m^3
Φ	viscous dissipation function, 1/s^2

ACKNOWLEDGEMENTS

The support of the University of Auckland Research Committee is gratefully acknowledged.

REFERENCES

1. Ghia U, Ghia KN, Shin CT. High-*Re* solutions for incompressible flow using the Navier–Stokes equations and a multigrid method. *Journal of Computational Physics* 1982; **48**:387–411.
2. Shen J. Hopf bifurcation of the unsteady regularized driven cavity. *Journal of Computational Physics* 1991; **95**:228–245.
3. de Vahl Davis G. Natural convection of air in a square cavity: a bench mark numerical solution. *International Journal for Numerical Methods in Fluids* 1983; **3**:249–264.
4. Bejan A. *Entropy Generation Through Heat and Fluid Flow*. Wiley: New York, 1982.
5. Aris R. *Vectors, Tensors and the Basic Equations of Fluid Mechanics*. Dover: Dordrecht, 1989.
6. Batchelor GK. *An Introduction to Fluid Dynamics*. Cambridge University Press: Cambridge, 1967.
7. Narusawa U. The second-law analysis of convection pattern change in a rectangular cavity. *Journal of Fluid Mechanics* 1999; **392**:361–377.
8. Norris SE. A parallel Navier–Stokes solver for natural convection and free surface flow. *Ph.D. Thesis*, University of Sydney, 2000.
9. Patankar SV. *Numerical Heat Transfer and Fluid Flow*. Hemisphere: New York, 1980.

Copyright © 2007 John Wiley & Sons, Ltd.

DOI: 10.1002/fld

10. Rhie CM, Chow WL. Numerical study of the turbulent flow past an airfoil with trailing edge separation. *AIAA Journal* 1983; **21**(11):1525–1532.
11. Were CJ. The free-ALE method for unsteady incompressible flow in deforming geometries. *Ph.D. Thesis*, University of Auckland, 1996.
12. Harlow FH, Welch JE. Numerical calculation of time-dependent viscous incompressible flow of fluid with a free surface. *Physics of Fluids* 1965; **8**:2182–2189.
13. Celik IB. Procedure for estimation and reporting of discretisation error in CFD applications, www.asme.org/pubs/journals/fluideng/JFENumAccuracy.pdf

Copyright © 2007 John Wiley & Sons, Ltd.

DOI: 10.1002/fld